

PDF hosted at the Radboud Repository of the Radboud University Nijmegen

The following full text is a publisher's version.

For additional information about this publication click this link.

<http://hdl.handle.net/2066/128804>

Please be advised that this information was generated on 2017-12-05 and may be subject to change.

Measurement of branching fractions and CP and isospin asymmetries for $B \rightarrow K^* \gamma$

B. Aubert,¹ R. Barate,¹ D. Boutigny,¹ F. Couderc,¹ J.-M. Gaillard,¹ A. Hicheur,¹ Y. Karyotakis,¹ J. P. Lees,¹ V. Tisserand,¹ A. Zghiche,¹ A. Palano,² A. Pompili,² J. C. Chen,³ N. D. Qi,³ G. Rong,³ P. Wang,³ Y. S. Zhu,³ G. Eigen,⁴ I. Ofte,⁴ B. Stugu,⁴ G. S. Abrams,⁵ A. W. Borgland,⁵ A. B. Breon,⁵ D. N. Brown,⁵ J. Button-Shafer,⁵ R. N. Cahn,⁵ E. Charles,⁵ C. T. Day,⁵ M. S. Gill,⁵ A. V. Gritsan,⁵ Y. Groysman,⁵ R. G. Jacobsen,⁵ R. W. Kadel,⁵ J. Kadyk,⁵ L. T. Kerth,⁵ Yu. G. Kolomensky,⁵ G. Kukartsev,⁵ G. Lynch,⁵ L. M. Mir,⁵ P. J. Oddone,⁵ T. J. Orimoto,⁵ M. Pripstein,⁵ N. A. Roe,⁵ M. T. Ronan,⁵ V. G. Shelkov,⁵ W. A. Wenzel,⁵ M. Barrett,⁶ K. E. Ford,⁶ T. J. Harrison,⁶ A. J. Hart,⁶ C. M. Hawkes,⁶ S. E. Morgan,⁶ A. T. Watson,⁶ M. Fritsch,⁷ K. Goetzen,⁷ T. Held,⁷ H. Koch,⁷ B. Lewandowski,⁷ M. Pelizaeus,⁷ M. Steinke,⁷ J. T. Boyd,⁸ N. Chevalier,⁸ W. N. Cottingham,⁸ M. P. Kelly,⁸ T. E. Latham,⁸ F. F. Wilson,⁸ T. Cuhadar-Donszelmann,⁹ C. Hearty,⁹ N. S. Knecht,⁹ T. S. Mattison,⁹ J. A. McKenna,⁹ D. Thiessen,⁹ A. Khan,¹⁰ P. Kyberd,¹⁰ L. Teodorescu,¹⁰ A. E. Blinov,¹¹ V. E. Blinov,¹¹ V. P. Druzhinin,¹¹ V. B. Golubev,¹¹ V. N. Ivanchenko,¹¹ E. A. Kravchenko,¹¹ A. P. Onuchin,¹¹ S. I. Serednyakov,¹¹ Yu. I. Skovpen,¹¹ E. P. Solodov,¹¹ A. N. Yushkov,¹¹ D. Best,¹² M. Bruinsma,¹² M. Chao,¹² I. Eschrich,¹² D. Kirkby,¹² A. J. Lankford,¹² M. Mandelkern,¹² R. K. Mommsen,¹² W. Roethel,¹² D. P. Stoker,¹² C. Buchanan,¹³ B. L. Hartfiel,¹³ S. D. Foulkes,¹⁴ J. W. Gary,¹⁴ B. C. Shen,¹⁴ K. Wang,¹⁴ D. del Re,¹⁵ H. K. Hadavand,¹⁵ E. J. Hill,¹⁵ D. B. MacFarlane,¹⁵ H. P. Paar,¹⁵ Sh. Rahatlou,¹⁵ V. Sharma,¹⁵ J. W. Berryhill,¹⁶ C. Campagnari,¹⁶ B. Dahmes,¹⁶ S. L. Levy,¹⁶ O. Long,¹⁶ A. Lu,¹⁶ M. A. Mazur,¹⁶ J. D. Richman,¹⁶ W. Verkerke,¹⁶ T. W. Beck,¹⁷ A. M. Eisner,¹⁷ C. A. Heusch,¹⁷ W. S. Lockman,¹⁷ G. Nesom,¹⁷ T. Schalk,¹⁷ R. E. Schmitz,¹⁷ B. A. Schumm,¹⁷ A. Seiden,¹⁷ P. Spradlin,¹⁷ D. C. Williams,¹⁷ M. G. Wilson,¹⁷ J. Albert,¹⁸ E. Chen,¹⁸ G. P. Dubois-Felsmann,¹⁸ A. Dvoretzskii,¹⁸ D. G. Hitlin,¹⁸ I. Narsky,¹⁸ T. Piatenko,¹⁸ F. C. Porter,¹⁸ A. Ryd,¹⁸ A. Samuel,¹⁸ S. Yang,¹⁸ S. Jayatilleke,¹⁹ G. Mancinelli,¹⁹ B. T. Meadows,¹⁹ M. D. Sokoloff,¹⁹ T. Abe,²⁰ F. Blanc,²⁰ P. Bloom,²⁰ S. Chen,²⁰ W. T. Ford,²⁰ U. Nauenberg,²⁰ A. Olivas,²⁰ P. Rankin,²⁰ J. G. Smith,²⁰ J. Zhang,²⁰ L. Zhang,²⁰ A. Chen,²¹ J. L. Harton,²¹ A. Soffer,²¹ W. H. Toki,²¹ R. J. Wilson,²¹ Q. L. Zeng,²¹ D. Altenburg,²² T. Brandt,²² J. Brose,²² M. Dickopp,²² E. Feltresi,²² A. Hauke,²² H. M. Lacker,²² R. Müller-Pfefferkorn,²² R. Nogowski,²² S. Otto,²² A. Petzold,²² J. Schubert,²² K. R. Schubert,²² R. Schwierz,²² B. Spaan,²² J. E. Sundermann,²² D. Bernard,²³ G. R. Bonneaud,²³ F. Brochard,²³ P. Grenier,²³ S. Schrenk,²³ Ch. Thiebaux,²³ G. Vasileiadis,²³ M. Verderi,²³ D. J. Bard,²⁴ P. J. Clark,²⁴ D. Lavin,²⁴ F. Muheim,²⁴ S. Playfer,²⁴ Y. Xie,²⁴ M. Andreotti,²⁵ V. Azzolini,²⁵ D. Bettoni,²⁵ C. Bozzi,²⁵ R. Calabrese,²⁵ G. Cibinetto,²⁵ E. Luppi,²⁵ M. Negrini,²⁵ L. Piemontese,²⁵ A. Sarti,²⁵ E. Treadwell,²⁶ R. Baldini-Ferrolì,²⁷ A. Calcaterra,²⁷ R. de Sangro,²⁷ G. Finocchiaro,²⁷ P. Patteri,²⁷ M. Piccolo,²⁷ A. Zallo,²⁷ A. Buzzo,²⁸ R. Capra,²⁸ R. Contri,²⁸ G. Crosetti,²⁸ M. Lo Vetere,²⁸ M. Macri,²⁸ M. R. Monge,²⁸ S. Passaggio,²⁸ C. Patrignani,²⁸ E. Robutti,²⁸ A. Santroni,²⁸ S. Tosi,²⁸ S. Bailey,²⁹ G. Brandenburg,²⁹ M. Morii,²⁹ E. Won,²⁹ R. S. Dubitzky,³⁰ U. Langenegger,³⁰ W. Bhimji,³¹ D. A. Bowerman,³¹ P. D. Dauncey,³¹ U. Egede,³¹ J. R. Gaillard,³¹ G. W. Morton,³¹ J. A. Nash,³¹ M. B. Nikolich,³¹ G. P. Taylor,³¹ M. J. Charles,³² G. J. Grenier,³² U. Mallik,³² J. Cochran,³³ H. B. Crawley,³³ J. Lamsa,³³ W. T. Meyer,³³ S. Prell,³³ E. I. Rosenberg,³³ J. Yi,³³ M. Davier,³⁴ G. Grosdidier,³⁴ A. Höcker,³⁴ S. Laplace,³⁴ F. Le Diberder,³⁴ V. Lepeltier,³⁴ A. M. Lutz,³⁴ T. C. Petersen,³⁴ S. Plaszczynski,³⁴ M. H. Schune,³⁴ L. Tantot,³⁴ G. Wormser,³⁴ C. H. Cheng,³⁵ D. J. Lange,³⁵ M. C. Simani,³⁵ D. M. Wright,³⁵ A. J. Bevan,³⁶ C. A. Chavez,³⁶ J. P. Coleman,³⁶ I. J. Forster,³⁶ J. R. Fry,³⁶ E. Gabathuler,³⁶ R. Gamet,³⁶ R. J. Parry,³⁶ D. J. Payne,³⁶ R. J. Sloane,³⁶ C. Touramanis,³⁶ J. J. Back,^{37,*} C. M. Cormack,³⁷ P. F. Harrison,^{37,*} F. Di Lodovico,³⁷ G. B. Mohanty,^{37,*} C. L. Brown,³⁸ G. Cowan,³⁸ R. L. Flack,³⁸ H. U. Flaecher,³⁸ M. G. Green,³⁸ P. S. Jackson,³⁸ T. R. McMahon,³⁸ S. Ricciardi,³⁸ F. Salvatore,³⁸ M. A. Winter,³⁸ D. Brown,³⁹ C. L. Davis,³⁹ J. Allison,⁴⁰ N. R. Barlow,⁴⁰ R. J. Barlow,⁴⁰ M. C. Hodgkinson,⁴⁰ G. D. Lafferty,⁴⁰ A. J. Lyon,⁴⁰ J. C. Williams,⁴⁰ A. Farbin,⁴¹ W. D. Hulsbergen,⁴¹ A. Jawahery,⁴¹ D. Kovalskyi,⁴¹ C. K. Lae,⁴¹ V. Lillard,⁴¹ D. A. Roberts,⁴¹ G. Blaylock,⁴² C. Dallapiccola,⁴² K. T. Flood,⁴² S. S. Hertzbach,⁴² K. Koeneke,⁴² R. Kofler,⁴² V. B. Koptchev,⁴² T. B. Moore,⁴² S. Saremi,⁴² H. Staengle,⁴² S. Willocq,⁴² R. Cowan,⁴³ G. Sciolla,⁴³ F. Taylor,⁴³ R. K. Yamamoto,⁴³ D. J. J. Mangeol,⁴⁴ P. M. Patel,⁴⁴ S. H. Robertson,⁴⁴ A. Lazzaro,⁴⁵ F. Palombo,⁴⁵ J. M. Bauer,⁴⁶ L. Cremaldi,⁴⁶ V. Eschenburg,⁴⁶ R. Godang,⁴⁶ R. Kroeger,⁴⁶ J. Reidy,⁴⁶ D. A. Sanders,⁴⁶ D. J. Summers,⁴⁶ H. W. Zhao,⁴⁶ S. Brunet,⁴⁷ D. Côté,⁴⁷ P. Taras,⁴⁷ H. Nicholson,⁴⁸ F. Fabozzi,^{49,†} C. Gatto,⁴⁹ L. Lista,⁴⁹ D. Monorchio,⁴⁹ P. Paolucci,⁴⁹ D. Piccolo,⁴⁹ C. Sciacca,⁴⁹ M. Baak,⁵⁰ H. Bulten,⁵⁰ G. Raven,⁵⁰ H. L. Snoek,⁵⁰ L. Wilden,⁵⁰ C. P. Jessop,⁵¹ J. M. LoSecco,⁵¹ T. A. Gabriel,⁵² T. Allmendinger,⁵³ B. Brau,⁵³ K. K. Gan,⁵³ K. Honscheid,⁵³ D. Hufnagel,⁵³ H. Kagan,⁵³ R. Kass,⁵³ T. Pulliam,⁵³ A. M. Rahimi,⁵³ R. Ter-Antonyan,⁵³ Q. K. Wong,⁵³ J. Brau,⁵⁴ R. Frey,⁵⁴ O. Igonkina,⁵⁴ C. T. Potter,⁵⁴ N. B. Sinev,⁵⁴ D. Strom,⁵⁴ E. Torrence,⁵⁴ F. Coleccchia,⁵⁵ A. Dorigo,⁵⁵ F. Galeazzi,⁵⁵ M. Margoni,⁵⁵ M. Morandin,⁵⁵ M. Posocco,⁵⁵ M. Rotondo,⁵⁵ F. Simonetto,⁵⁵ R. Stroili,⁵⁵ G. Tiozzo,⁵⁵ C. Voci,⁵⁵ M. Benayoun,⁵⁶ H. Briand,⁵⁶ J. Chauveau,⁵⁶ P. David,⁵⁶

Ch. de la Vaissière,⁵⁶ L. Del Buono,⁵⁶ O. Hamon,⁵⁶ M. J. J. John,⁵⁶ Ph. Leruste,⁵⁶ J. Malcles,⁵⁶ J. Ocariz,⁵⁶ M. Pivk,⁵⁶ L. Roos,⁵⁶ S. T'Jampens,⁵⁶ G. Therin,⁵⁶ P. F. Manfredi,⁵⁷ V. Re,⁵⁷ P. K. Behera,⁵⁸ L. Gladney,⁵⁸ Q. H. Guo,⁵⁸ J. Panetta,⁵⁸ F. Anulli,^{27,59} M. Biasini,⁵⁹ I. M. Peruzzi,^{27,59} M. Pioppi,⁵⁹ C. Angelini,⁶⁰ G. Batignani,⁶⁰ S. Bettarini,⁶⁰ M. Bondioli,⁶⁰ F. Bucci,⁶⁰ G. Calderini,⁶⁰ M. Carpinelli,⁶⁰ F. Forti,⁶⁰ M. A. Giorgi,⁶⁰ A. Lusiani,⁶⁰ G. Marchiori,⁶⁰ F. Martinez-Vidal,^{60,‡} M. Morganti,⁶⁰ N. Neri,⁶⁰ E. Paoloni,⁶⁰ M. Rama,⁶⁰ G. Rizzo,⁶⁰ F. Sandrelli,⁶⁰ J. Walsh,⁶⁰ M. Haire,⁶¹ D. Judd,⁶¹ K. Paick,⁶¹ D. E. Wagoner,⁶¹ N. Danielson,⁶² P. Elmer,⁶² Y. P. Lau,⁶² C. Lu,⁶² V. Miftakov,⁶² J. Olsen,⁶² A. J. S. Smith,⁶² A. V. Telnov,⁶² F. Bellini,⁶³ G. Cavoto,^{62,63} R. Faccini,⁶³ F. Ferrarotto,⁶³ F. Ferroni,⁶³ M. Gaspero,⁶³ L. Li Gioi,⁶³ M. A. Mazzoni,⁶³ S. Morganti,⁶³ M. Pierini,⁶³ G. Piredda,⁶³ F. Safai Tehrani,⁶³ C. Voena,⁶³ S. Christ,⁶⁴ G. Wagner,⁶⁴ R. Waldi,⁶⁴ T. Adye,⁶⁵ N. De Groot,⁶⁵ B. Franek,⁶⁵ N. I. Geddes,⁶⁵ G. P. Gopal,⁶⁵ E. O. Olaiya,⁶⁵ R. Aleksan,⁶⁶ S. Emery,⁶⁶ A. Gaidot,⁶⁶ S. F. Ganzhur,⁶⁶ P.-F. Giraud,⁶⁶ G. Hamel de Monchenault,⁶⁶ W. Kozanecki,⁶⁶ M. Langer,⁶⁶ M. Legendre,⁶⁶ G. W. London,⁶⁶ B. Mayer,⁶⁶ G. Schott,⁶⁶ G. Vasseur,⁶⁶ Ch. Yèche,⁶⁶ M. Zito,⁶⁶ M. V. Purohit,⁶⁷ A. W. Weidemann,⁶⁷ J. R. Wilson,⁶⁷ F. X. Yumiceva,⁶⁷ D. Aston,⁶⁸ R. Bartoldus,⁶⁸ N. Berger,⁶⁸ A. M. Boyarski,⁶⁸ O. L. Buchmueller,⁶⁸ R. Claus,⁶⁸ M. R. Convery,⁶⁸ M. Cristinziani,⁶⁸ G. De Nardo,⁶⁸ D. Dong,⁶⁸ J. Dorfan,⁶⁸ D. Dujmic,⁶⁸ W. Dunwoodie,⁶⁸ E. E. Elsen,⁶⁸ S. Fan,⁶⁸ R. C. Field,⁶⁸ T. Glanzman,⁶⁸ S. J. Gowdy,⁶⁸ T. Hadig,⁶⁸ V. Halyo,⁶⁸ C. Hast,⁶⁸ T. Hryn'ova,⁶⁸ W. R. Innes,⁶⁸ M. H. Kelsey,⁶⁸ P. Kim,⁶⁸ M. L. Kocian,⁶⁸ D. W. G. S. Leith,⁶⁸ J. Libby,⁶⁸ S. Luitz,⁶⁸ V. Luth,⁶⁸ H. L. Lynch,⁶⁸ H. Marsiske,⁶⁸ R. Messner,⁶⁸ D. R. Muller,⁶⁸ C. P. O'Grady,⁶⁸ V. E. Ozcan,⁶⁸ A. Perazzo,⁶⁸ M. Perl,⁶⁸ S. Petrak,⁶⁸ B. N. Ratcliff,⁶⁸ A. Roodman,⁶⁸ A. A. Salnikov,⁶⁸ R. H. Schindler,⁶⁸ J. Schwiening,⁶⁸ G. Simi,⁶⁸ A. Snyder,⁶⁸ A. Soha,⁶⁸ J. Stelzer,⁶⁸ D. Su,⁶⁸ M. K. Sullivan,⁶⁸ J. Va'vra,⁶⁸ S. R. Wagner,⁶⁸ M. Weaver,⁶⁸ A. J. R. Weinstein,⁶⁸ W. J. Wisniewski,⁶⁸ M. Wittgen,⁶⁸ D. H. Wright,⁶⁸ A. K. Yarritu,⁶⁸ C. C. Young,⁶⁸ P. R. Burchat,⁶⁹ A. J. Edwards,⁶⁹ T. I. Meyer,⁶⁹ B. A. Petersen,⁶⁹ C. Roat,⁶⁹ S. Ahmed,⁷⁰ M. S. Alam,⁷⁰ J. A. Ernst,⁷⁰ M. A. Saeed,⁷⁰ M. Saleem,⁷⁰ F. R. Wappler,⁷⁰ W. Bugg,⁷¹ M. Krishnamurthy,⁷¹ S. M. Spanier,⁷¹ R. Eckmann,⁷² H. Kim,⁷² J. L. Ritchie,⁷² A. Satpathy,⁷² R. F. Schwitters,⁷² J. M. Izen,⁷³ I. Kitayama,⁷³ X. C. Lou,⁷³ S. Ye,⁷³ F. Bianchi,⁷⁴ M. Bona,⁷⁴ F. Gallo,⁷⁴ D. Gamba,⁷⁴ C. Borean,⁷⁵ L. Bosisio,⁷⁵ C. Cartaro,⁷⁵ F. Cossutti,⁷⁵ G. Della Ricca,⁷⁵ S. Dittongo,⁷⁵ S. Grancagnolo,⁷⁵ L. Lanceri,⁷⁵ P. Poropat,^{75,§} L. Vitale,⁷⁵ G. Vuagnin,⁷⁵ R. S. Panvini,⁷⁶ Sw. Banerjee,⁷⁷ C. M. Brown,⁷⁷ D. Fortin,⁷⁷ P. D. Jackson,⁷⁷ R. Kowalewski,⁷⁷ J. M. Roney,⁷⁷ R. J. Sobie,⁷⁷ H. R. Band,⁷⁸ S. Dasu,⁷⁸ M. Datta,⁷⁸ A. M. Eichenbaum,⁷⁸ M. Graham,⁷⁸ J. J. Hollar,⁷⁸ J. R. Johnson,⁷⁸ P. E. Kutter,⁷⁸ H. Li,⁷⁸ R. Liu,⁷⁸ A. Mihalyi,⁷⁸ A. K. Mohapatra,⁷⁸ Y. Pan,⁷⁸ R. Prepost,⁷⁸ A. E. Rubin,⁷⁸ S. J. Sekula,⁷⁸ P. Tan,⁷⁸ J. H. von Wimmersperg-Toeller,⁷⁸ J. Wu,⁷⁸ S. L. Wu,⁷⁸ Z. Yu,⁷⁸ M. G. Greene,⁷⁹ and H. Neal⁷⁹

(BABAR Collaboration)

¹Laboratoire de Physique des Particules, F-74941 Annecy-le-Vieux, France

²Università di Bari, Dipartimento di Fisica and INFN, I-70126 Bari, Italy

³Institute of High Energy Physics, Beijing 100039, China

⁴Institute of Physics, University of Bergen, N-5007 Bergen, Norway

⁵Lawrence Berkeley National Laboratory and University of California, Berkeley, California 94720, USA

⁶University of Birmingham, Birmingham, B15 2TT, United Kingdom

⁷Institut für Experimentalphysik 1, Ruhr Universität Bochum, D-44780 Bochum, Germany

⁸University of Bristol, Bristol BS8 1TL, United Kingdom

⁹University of British Columbia, Vancouver, BC, Canada V6T 1Z1

¹⁰Brunel University, Uxbridge, Middlesex UB8 3PH, United Kingdom

¹¹Budker Institute of Nuclear Physics, Novosibirsk 630090, Russia

¹²University of California at Irvine, Irvine, California 92697, USA

¹³University of California at Los Angeles, Los Angeles, California 90024, USA

¹⁴University of California at Riverside, Riverside, California 92521, USA

¹⁵University of California at San Diego, La Jolla, California 92093, USA

¹⁶University of California at Santa Barbara, Santa Barbara, California 93106, USA

¹⁷Institute for Particle Physics, University of California at Santa Cruz, Santa Cruz, California 95064, USA

¹⁸California Institute of Technology, Pasadena, California 91125, USA

¹⁹University of Cincinnati, Cincinnati, Ohio 45221, USA

²⁰University of Colorado, Boulder, Colorado 80309, USA

²¹Colorado State University, Fort Collins, Colorado 80523, USA

²²Institut für Kern- und Teilchenphysik, Technische Universität Dresden, D-01062 Dresden, Germany

²³Ecole Polytechnique, LLR, F-91128 Palaiseau, France

²⁴University of Edinburgh, Edinburgh EH9 3JZ, United Kingdom

- ²⁵*Università di Ferrara, Dipartimento di Fisica and INFN, I-44100 Ferrara, Italy*
²⁶*Florida A&M University, Tallahassee, Florida 32307, USA*
²⁷*Laboratori Nazionali di Frascati dell'INFN, I-00044 Frascati, Italy*
²⁸*Università di Genova, Dipartimento di Fisica and INFN, I-16146 Genova, Italy*
²⁹*Harvard University, Cambridge, Massachusetts 02138, USA*
³⁰*Physikalisches Institut, Universität Heidelberg, Philosophenweg 12, D-69120 Heidelberg, Germany*
³¹*Imperial College London, London, SW7 2AZ, United Kingdom*
³²*University of Iowa, Iowa City, Iowa 52242, USA*
³³*Iowa State University, Ames, Iowa 50011-3160, USA*
³⁴*Laboratoire de l'Accélérateur Linéaire, F-91898 Orsay, France*
³⁵*Lawrence Livermore National Laboratory, Livermore, California 94550, USA*
³⁶*University of Liverpool, Liverpool L69 7ZE, United Kingdom*
³⁷*Queen Mary, University of London, E1 4NS, United Kingdom*
³⁸*Royal Holloway and Bedford New College, University of London, Egham, Surrey TW20 0EX, United Kingdom*
³⁹*University of Louisville, Louisville, Kentucky 40292, USA*
⁴⁰*University of Manchester, Manchester M13 9PL, United Kingdom*
⁴¹*University of Maryland, College Park, Maryland 20742, USA*
⁴²*University of Massachusetts, Amherst, Massachusetts 01003, USA*
⁴³*Laboratory for Nuclear Science, Massachusetts Institute of Technology, Cambridge, Massachusetts 02139, USA*
⁴⁴*McGill University, Montréal, QC, Canada H3A 2T8*
⁴⁵*Università di Milano, Dipartimento di Fisica and INFN, I-20133 Milano, Italy*
⁴⁶*University of Mississippi, University, Mississippi 38677, USA*
⁴⁷*Laboratoire René J. A. Lévesque, Université de Montréal, Montréal, QC, Canada H3C 3J7*
⁴⁸*Mount Holyoke College, South Hadley, Massachusetts 01075, USA*
⁴⁹*Università di Napoli Federico II, Dipartimento di Scienze Fisiche and INFN, I-80126, Napoli, Italy*
⁵⁰*NIKHEF, National Institute for Nuclear Physics and High Energy Physics, NL-1009 DB Amsterdam, The Netherlands*
⁵¹*University of Notre Dame, Notre Dame, Indiana 46556, USA*
⁵²*Oak Ridge National Laboratory, Oak Ridge, Tennessee 37831, USA*
⁵³*The Ohio State University, Columbus, Ohio 43210, USA*
⁵⁴*University of Oregon, Eugene, Oregon 97403, USA*
⁵⁵*Università di Padova, Dipartimento di Fisica and INFN, I-35131 Padova, Italy*
⁵⁶*Laboratoire de Physique Nucléaire et de Hautes Energies, Universités Paris VI et VII, F-75252 Paris, France*
⁵⁷*Università di Pavia, Dipartimento di Elettronica and INFN, I-27100 Pavia, Italy*
⁵⁸*University of Pennsylvania, Philadelphia, Pennsylvania 19104, USA*
⁵⁹*Università di Perugia, Dipartimento di Fisica and INFN, I-06100 Perugia, Italy*
⁶⁰*Università di Pisa, Dipartimento di Fisica, Scuola Normale Superiore and INFN, I-56127 Pisa, Italy*
⁶¹*Prairie View A&M University, Prairie View, Texas 77446, USA*
⁶²*Princeton University, Princeton, New Jersey 08544, USA*
⁶³*Università di Roma La Sapienza, Dipartimento di Fisica and INFN, I-00185 Roma, Italy*
⁶⁴*Universität Rostock, D-18051 Rostock, Germany*
⁶⁵*Rutherford Appleton Laboratory, Chilton, Didcot, Oxon, OX11 0QX, United Kingdom*
⁶⁶*DSM/Dapnia, CEA/Saclay, F-91191 Gif-sur-Yvette, France*
⁶⁷*University of South Carolina, Columbia, South Carolina 29208, USA*
⁶⁸*Stanford Linear Accelerator Center, Stanford, California 94309, USA*
⁶⁹*Stanford University, Stanford, California 94305-4060, USA*
⁷⁰*State University of New York, Albany, New York 12222, USA*
⁷¹*University of Tennessee, Knoxville, Tennessee 37996, USA*
⁷²*University of Texas at Austin, Austin, Texas 78712, USA*
⁷³*University of Texas at Dallas, Richardson, Texas 75083, USA*
⁷⁴*Università di Torino, Dipartimento di Fisica Sperimentale and INFN, I-10125 Torino, Italy*
⁷⁵*Università di Trieste, Dipartimento di Fisica and INFN, I-34127 Trieste, Italy*
⁷⁶*Vanderbilt University, Nashville, Tennessee 37235, USA*
⁷⁷*University of Victoria, Victoria, BC, Canada V8W 3P6*
⁷⁸*University of Wisconsin, Madison, Wisconsin 53706, USA*
⁷⁹*Yale University, New Haven, Connecticut 06511, USA*
(Received 30 June 2004; published 21 December 2004)

The branching fractions of the decays $B^0 \rightarrow K^{*0} \gamma$ and $B^+ \rightarrow K^{*+} \gamma$ are measured using a sample of $88 \times 10^6 B\bar{B}$ events collected with the BABAR detector at the PEP-II asymmetric-energy e^+e^- collider. We find $\mathcal{B}(B^0 \rightarrow K^{*0} \gamma) = [3.92 \pm 0.20(\text{stat}) \pm 0.24(\text{syst})] \times 10^{-5}$, $\mathcal{B}(B^+ \rightarrow K^{*+} \gamma) = [3.87 \pm 0.28(\text{stat}) \pm 0.26(\text{syst})] \times 10^{-5}$. Our measurements also constrain the direct CP asymmetry to be

$-0.074 < \mathcal{A}(B \rightarrow K^* \gamma) < 0.049$ and the isospin asymmetry to be $-0.046 < \Delta_{0-} < 0.146$, both at the 90% confidence level.

DOI: 10.1103/PhysRevD.70.112006

PACS numbers: 13.20.He, 11.30.Er

Within the standard model (SM), the decays $B \rightarrow K^* \gamma$ proceed dominantly through one-loop $b \rightarrow s \gamma$ electromagnetic ‘‘penguin’’ transitions [1]. Non-SM virtual particles may be present in these loops, changing the decay rates from the SM predictions. Theoretical calculations of exclusive $B \rightarrow K^* \gamma$ decay rates have large uncertainties due to nonperturbative hadronic effects [2–4], limiting their usefulness for probing new physics. Previous measurements [5–7] of the branching fractions are already more precise than SM-based theoretical estimates and are in reasonable agreement with them. Calculations [8,9] of the form factor for $B \rightarrow K^* \gamma$ can be tested using improved measurements of these branching fractions.

Much of the theoretical uncertainty in the branching fractions cancels in the ratios defining the isospin asymmetry Δ_{0-} and the CP asymmetry \mathcal{A} :

$$\Delta_{0-} = \frac{\Gamma(\bar{B}^0 \rightarrow \bar{K}^{*0} \gamma) - \Gamma(B^- \rightarrow K^{*-} \gamma)}{\Gamma(\bar{B}^0 \rightarrow \bar{K}^{*0} \gamma) + \Gamma(B^- \rightarrow K^{*-} \gamma)}, \quad (1)$$

$$\mathcal{A} = \frac{\Gamma(\bar{B} \rightarrow \bar{K}^* \gamma) - \Gamma(B \rightarrow K^* \gamma)}{\Gamma(\bar{B} \rightarrow \bar{K}^* \gamma) + \Gamma(B \rightarrow K^* \gamma)}, \quad (2)$$

making them stringent tests of the SM. A further advantage of these asymmetries is that some experimental systematic uncertainties cancel in the ratios. The SM predicts a positive value of Δ_{0-} between 5% and 10% [10] and $|\mathcal{A}|$ less than 1% [11]. New physics contributions can modify these values significantly [10,11].

In this paper, we present measurements of the exclusive branching fractions $\mathcal{B}(B^0 \rightarrow K^{*0} \gamma)$ and $\mathcal{B}(B^+ \rightarrow K^{*+} \gamma)$, the isospin asymmetry (Δ_{0-}), and the CP asymmetries $\mathcal{A}(B^0 \rightarrow K^{*0} \gamma)$ and $\mathcal{A}(B^+ \rightarrow K^{*+} \gamma)$. K^* refers to the $K^*(892)$ resonance throughout this paper. Inclusion of charge-conjugate decays is implied except in the definitions of \mathcal{A} . This analysis uses $(88 \pm 1) \times 10^6 B\bar{B}$ events, from $Y(4S)$ decays, recorded by the *BABAR* detector [12]. An additional 10 fb^{-1} of data, taken 40 MeV below the $Y(4S)$ resonance, is used for studying non- B continuum background. After $B \rightarrow K^* \gamma$ event reconstruction and background rejection, multidimensional extended maximum likelihood fits are used to extract the final results.

We reconstruct $B^0 \rightarrow K^{*0} \gamma$ in the $K^{*0} \rightarrow K^+ \pi^-$, $K_S^0 \pi^0$ modes and $B^+ \rightarrow K^{*+} \gamma$ in the $K^{*+} \rightarrow K^+ \pi^0$, $K_S^0 \pi^+$

modes as described in detail in Refs. [6,12]. Reconstructed tracks are identified as final state π^\pm and K^\pm mesons by measuring the angle of the Cherenkov cone and energy loss along the track (dE/dx). The K_S^0 candidates are composed from pairs of oppositely charged tracks with an invariant mass that is within 3.3σ of the nominal K_S^0 mass and with a vertex that is at least 0.3 cm away from the primary event vertex. The π^0 -candidate momentum vector is determined by a mass-constrained fit to pairs of photons, reconstructed from energy deposits in the calorimeter that are not matched to tracks. The K and π candidates are combined to form K^* candidates, which are required to have invariant mass in the range $800 < M_{K\pi} < 1000 \text{ MeV}/c^2$. The primary-photon candidates are required to have high center-of-mass (CM) energy, between 1.5 and 3.5 GeV, and to satisfy additional requirements designed to suppress the large π^0 and η background as described in Ref. [6].

The B -meson candidates are reconstructed by combining the K^* and high-energy photon candidates. We define in the CM frame (denoted by asterisks) $\Delta E^* \equiv E_B^* - E_{\text{beam}}^*$, where E_{beam}^* is the beam energy, known to high precision, and $E_B^* = E_\gamma^* + E_{K^*}^*$ is the energy of the B -meson candidate. We also define the beam-energy-substituted mass $m_{\text{ES}} \equiv \sqrt{E_{\text{beam}}^{*2} - p_B^{*2}}$, where p_B^* is the momentum of the B candidate modified by scaling the photon energy to make $E_\gamma^* + E_{K^*}^* - E_{\text{beam}}^* = 0$. This procedure reduces the tail in the signal m_{ES} distribution, which results from the asymmetric calorimeter response. For signal decays, this ‘‘rescaled’’ m_{ES} peaks near $5.279 \text{ GeV}/c^2$ with a resolution of $\approx 3 \text{ MeV}/c^2$ and ΔE^* peaks near 0 MeV with a resolution of $\approx 50 \text{ MeV}$. We consider only candidates with $m_{\text{ES}} > 5.20 \text{ GeV}/c^2$ and $|\Delta E^*| < 0.3 \text{ GeV}$.

Background events arise predominantly from random combinations of particles in $q\bar{q}$ production ($q = u, d, s, c$), with the high-energy photon originating from initial-state radiation or from π^0 and η decays. We suppress this jetlike background in favor of the spherical signal events, using several event-shape variables as in Ref. [6]. To maximize separation between signal and background, these variables are combined in neural networks that are separately optimized for each decay mode. Each network is trained using Monte Carlo (MC) events and is validated on statistically independent MC samples. Cuts are made on the neural-network output to suppress continuum background. The m_{ES} and ΔE^* distributions of data are shown in Fig. 1 for all four K^* decay modes.

The remaining background includes that from $B\bar{B}$ events, which is dominated by $B \rightarrow X_s \gamma$ decays, where

*Present address: Department of Physics, University of Warwick, Coventry, United Kingdom.

†Also at Università della Basilicata, Potenza, Italy.

‡Also at IFIC, Instituto de Física Corpuscular, CSIC-Universidad de Valencia, Valencia, Spain.

§Deceased.

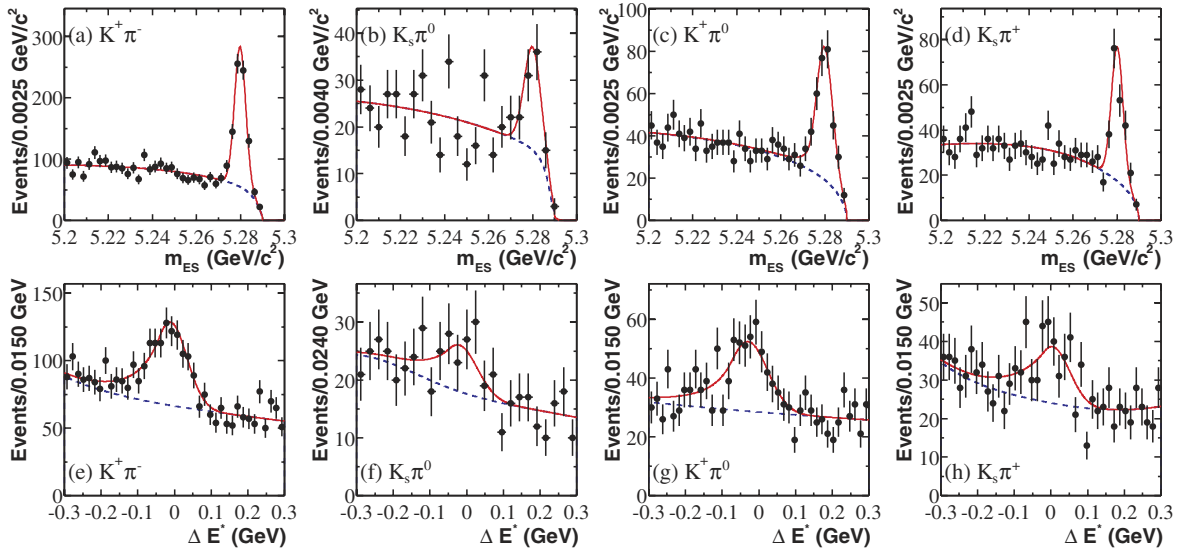


FIG. 1 (color online). m_{ES} and ΔE^* distributions for the $B \rightarrow K^* \gamma$ candidates. The points are data, and the solid and dashed curves show the projections of the complete fit and the background component alone, respectively. The fits used to extract the signal yields are described in the text.

X_s represents hadronic final states other than K^* . If one or more particles escape detection, X_s may be incorrectly reconstructed as K^* , leading to a value of m_{ES} near the B -meson mass, but with ΔE^* distinctly negative.

For each decay mode, the signal yield and asymmetry \mathcal{A} (except for the $K_s \pi^0$ mode) are simultaneously extracted using an extended unbinned maximum likelihood fit,

$$\mathcal{L} = \exp\left(-\sum_{i=1}^3 n_i\right) \left[\prod_{j=1}^N \sum_{i=1}^3 N_i \mathcal{P}(\vec{x}_j; \vec{\alpha}_i) \right],$$

to the two-dimensional distribution of m_{ES} and ΔE^* with three hypotheses (index i): signal, continuum background, and B background. The probability density function (PDF) $\mathcal{P}(\vec{x}_j; \vec{\alpha}_i)$ for each of the three hypotheses is the product of individual PDFs of the fit variables $\vec{x}_j = (m_{ES}, \Delta E^*)$. $\vec{\alpha}_i$ are the shape parameters for the PDFs described below. In the three self-flavor-tagged modes ($K^+ \pi^-$, $K^+ \pi^0$, and $K_s \pi^+$), $N_i = \frac{1}{2}(1 - \mathcal{F} \mathcal{A}_i)n_i$, where n_i and \mathcal{A}_i stand for the total yield and CP asymmetry of signal, continuum background, and B background, while in the $K_s \pi^0$ decay mode, $N_i = n_i$. The bottom-quark flavor \mathcal{F} is defined as -1 for b quarks and $+1$ for \bar{b} quarks. In the $K^+ \pi^-$ mode, mistagging is possible if both the pion and kaon are misidentified, but this probability is negligibly small. We assume that the CP asymmetry of the B background and that of the continuum background are the same.

To reduce systematic errors, most of the fit parameters for the signal and for the continuum background are determined by a fit to data. For continuum background, the ΔE^* distribution is modeled by a first-order polynomial

function with the exception of $K_s \pi^+$, where a second-order polynomial is used. The m_{ES} distribution for continuum background is modeled with an ARGUS function [13]. In the $K^+ \pi^0$ decay mode, the continuum background shape is simultaneously fit to the off-resonance data to obtain a stabler fit. For the B background, the Gaussian distribution

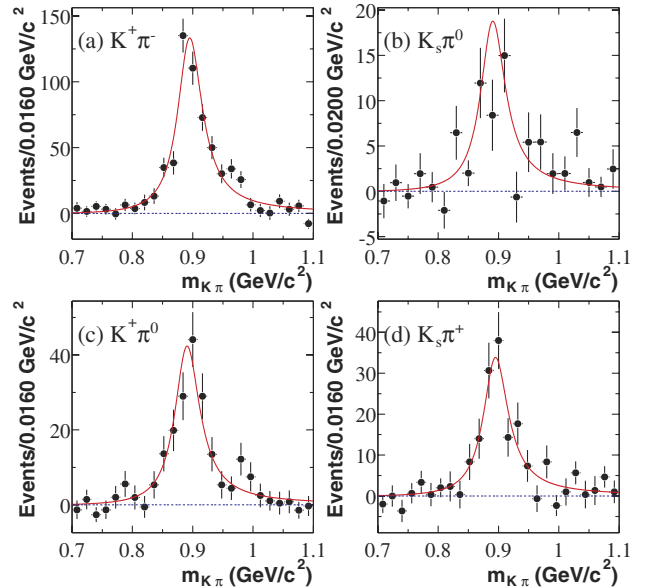


FIG. 2 (color online). $m_{K\pi}$ spectra for the different decay modes for events in the signal region after background subtraction using sidebands in m_{ES} and ΔE^* . The points are data and solid curves represent relativistic p -wave Breit-Wigner line shapes with masses and widths of K^* taken from Ref. [17].

TABLE I. The signal efficiency ϵ , the fitted signal yield N_S , the branching fraction \mathcal{B} , and the CP asymmetry \mathcal{A} for each decay mode. The combined branching fractions for $B^0 \rightarrow K^{*0}\gamma$ and $B^+ \rightarrow K^{*+}\gamma$, and combined CP asymmetry for all three modes studied, are also shown. Errors are statistical and systematic, with the exception of ϵ and N_S , which have only systematic and statistical errors, respectively. The detailed systematic errors are listed in Table II.

Mode	$\epsilon(\%)$	N_S	$\mathcal{B}(\times 10^{-5})$	Combined $\mathcal{B}(\times 10^{-5})$	\mathcal{A}	Combined \mathcal{A}
$K^+\pi^-$	24.4 ± 1.4	583 ± 30	$3.92 \pm 0.20 \pm 0.23$	$3.92 \pm 0.20 \pm 0.24$	$-0.069 \pm 0.046 \pm 0.011$	$-0.013 \pm 0.036 \pm 0.010$
$K_S^0\pi^0$	15.3 ± 1.9	62 ± 15	$4.02 \pm 0.99 \pm 0.51$			
$K^+\pi^0$	17.4 ± 1.6	251 ± 23	$4.90 \pm 0.45 \pm 0.46$	$3.87 \pm 0.28 \pm 0.26$	$0.084 \pm 0.075 \pm 0.007$	
$K_S^0\pi^+$	22.1 ± 1.4	157 ± 16	$3.52 \pm 0.35 \pm 0.22$			

used for ΔE^* and the Novosibirsk function [14] used for m_{ES} have all shape parameters fixed to values determined from MC. The signal ΔE^* distribution is modeled as a Crystal Ball function [15], which is a Gaussian distribution with a lowside power-law tail that is fixed using MC. The m_{ES} distribution for signal is modeled as a Gaussian function, except for the $K^+\pi^0$ decay mode, where a Crystal Ball function, with tail parameters fixed using MC fits, is used to accommodate a lowside tail due to the π^0 energy lost from the calorimeter. The same lowside tail in the $K_S^0\pi^0$ decay mode is ignored due to the small number of events in this mode.

Correlations between m_{ES} and ΔE^* distributions could introduce a bias in the signal yields. To study this, randomly selected events from our detailed MC simulation of the signal were mixed with background events generated using the PDF from the fit. In this way, we determined that the $K^+\pi^-$ efficiency must be corrected by multiplying it by 0.98. For the $K_S^0\pi^0$, $K^+\pi^0$, and $K_S^0\pi^+$ modes, the corresponding numbers are 0.91, 0.96, and 0.96. The error in this fit bias due to MC statistics is included as a systematic uncertainty. These MC studies also indicate that correlations between the B background and the continuum background fit yields do not affect the fitted signal yield.

The projections of the maximum likelihood fits on m_{ES} and ΔE^* are shown in Fig. 1 for each decay mode. Figure 2 shows that the background-subtracted $K\pi$ invariant mass distributions agree well with the expected K^* resonance shape. This confirms that the signal is consistent with coming from only true K^* decays.

Table I shows signal efficiencies, yields from the fits, and branching fractions (\mathcal{B}) calculated using our recent measurement [16] of the production ratio of charged and neutral B events, $R^{+/0} \equiv \Gamma(e^+e^- \rightarrow B^+B^-)/\Gamma(e^+e^- \rightarrow B^0\bar{B}^0) = 1.006 \pm 0.048$ at $\sqrt{s} = M_{Y(4S)}$.

Combined values of $\mathcal{B}(B^0 \rightarrow K^{*0}\gamma)$ and $\mathcal{B}(B^+ \rightarrow K^{*+}\gamma)$, which are also shown in Table I, are calculated taking into account correlated systematic errors between modes. We further combined these measurements, using the lifetime ratio $\tau_{B^+}/\tau_{B^0} = 1.083 \pm 0.017$ [17] and our measurement of $R^{+/0}$, to find the isospin asymmetry, $\Delta_{0-} = 0.050 \pm 0.045(\text{stat}) \pm 0.028(\text{syst}) \pm 0.024(R^{+/0})$, which corresponds to an allowed region of $-0.046 < \Delta_{0-} < 0.146$ at the 90% confidence level. We also present

a combined \mathcal{A} measurement in Table I, which corresponds to an allowed region of $-0.074 < \mathcal{A}(B \rightarrow K^*\gamma) < 0.049$ at the 90% confidence level.

The systematic error on the branching fraction for each mode is shown in Table II. Most of the uncertainties are determined as in our previous analysis [6], so we provide details only for the new procedures used. The neural-network inputs are generally independent of the fully reconstructed $B \rightarrow K^*\gamma$ candidate, so we determine their efficiencies and systematic uncertainties with high-purity control samples with reconstructed $B^- \rightarrow D^0\pi^-$ and $B^0 \rightarrow D^-\pi^+$. The ‘‘PDF parametrization’’ error comes from MC studies of our fitting procedure, in which we estimate the uncertainty incurred by fixing parameters in the continuum and B background models. This includes uncertainty in the inclusive branching fraction and spectral shape of $B \rightarrow X_s\gamma$.

The systematic uncertainties in the measurement of \mathcal{A} are also shown in Table II. The first three contributions arise from potential particle-antiparticle asymmetries in

TABLE II. Fractional systematic uncertainties on the branching fractions \mathcal{B} and absolute systematic uncertainties on CP asymmetry \mathcal{A} .

Description	Systematic errors on $\mathcal{B}(\%)$			
	$K^+\pi^-$	$K_S^0\pi^0$	$K^+\pi^0$	$K_S^0\pi^+$
Number of B events	1.1	1.1	1.1	1.1
$R^{+/0}$	2.4	2.4	2.4	2.4
Tracking efficiency	1.6		0.8	0.8
Charged particle identification	1.0		1.0	1.0
Photon efficiency	2.5	7.6	7.6	2.5
Photon isolation cut	2.0	2.0	2.0	2.0
π^0, η veto	1.0	1.0	1.0	1.0
K_S efficiency		3.0		3.0
Neural network	3.0	3.5	2.7	2.8
PDF parametrization	2.2	7.3	2.7	1.4
MC statistics/fit bias	0.9	3.2	2.4	1.6
Total	5.8	12.3	9.4	6.3
	Systematic errors on $\mathcal{A} (\%)$			
Tracking efficiency	0.35		0.25	0.25
Charged particle identification	1.00		0.55	0.53
Nuclear interaction asymmetry	0.20		0.35	0.15
B -background asymmetry	0.25		0.25	0.25
Total	1.1		0.7	0.7

the detector response, including differences in interaction cross sections for K^+ and K^- and for π^+ and π^- (estimated with a method similar to that used in Ref. [18]). The uncertainty due to a possible asymmetry in the B background, which is dominated by $B \rightarrow X_s \gamma$, is estimated by varying the background according to the uncertainty in our recent measurement of $\mathcal{A}(B \rightarrow X_s \gamma)$ [19].

We conclude that both the isospin and CP asymmetries in $B \rightarrow K^* \gamma$ decay processes are consistent with SM predictions. The branching fractions measured are also consistent with SM-based calculations and are more precise than those predictions. These measurements are consistent with previous results [5–7].

We are grateful for the excellent luminosity and machine conditions provided by our PEP-II colleagues and for the substantial dedicated effort from the computing organizations that support *BABAR*. The collaborating institutions thank SLAC for its support and kind hospitality. This work is supported by DOE and NSF (USA), NSERC (Canada), IHEP (China), CEA and CNRS-IN2P3 (France), BMBF and DFG (Germany), INFN (Italy), FOM (The Netherlands), NFR (Norway), MIST (Russia), and PPARC (United Kingdom). Individuals have received support from CONACyT (Mexico), A.P. Sloan Foundation, Research Corporation, and Alexander von Humboldt Foundation.

-
- [1] K. Lingel, T. Skwarnicki, and J. Smith, *Annu. Rev. Nucl. Part. Sci.* **48**, 253 (1998).
- [2] M. Beneke, T. Feldmann, and D. Seidel, *Nucl. Phys.* **B612**, 25 (2001).
- [3] S.W. Bosch and G. Buchalla, *Nucl. Phys.* **B621**, 459 (2002).
- [4] A. Ali and A.Y. Parkhomenko, *Eur. Phys. J. C* **23**, 89 (2002).
- [5] CLEO Collaboration, T.E. Coan *et al.*, *Phys. Rev. Lett.* **84**, 5283 (2000).
- [6] *BABAR* Collaboration, B. Aubert *et al.*, *Phys. Rev. Lett.* **88**, 101805 (2002).
- [7] Belle Collaboration, M. Nakao *et al.*, *Phys. Rev. D* **69**, 112001 (2004).
- [8] UKQCD Collaboration, L. Del Debbio, J.M. Flynn, L. Lellouch, and J. Nieves, *Phys. Lett. B* **416**, 392 (1998).
- [9] P. Ball and V.M. Braun, *Phys. Rev. D* **58**, 094016 (1998).
- [10] A.L. Kagan and M. Neubert, *Phys. Lett. B* **539**, 227 (2002).
- [11] A.L. Kagan and M. Neubert, *Phys. Rev. D* **58**, 094012 (1998).
- [12] *BABAR* Collaboration, B. Aubert *et al.*, *Nucl. Instrum. Methods Phys. Res., Sect. A* **479**, 1 (2002).
- [13] ARGUS Collaboration, H. Albrecht *et al.*, *Z. Phys. C* **48**, 543 (1990). See Sec. 3.1 for definition of ARGUS function.
- [14] The Novosibirsk function is defined as $f(m_{ES}) = A_S \exp(-0.5\{\ln^2[1 + \Lambda\tau(m_{ES} - m_0)]/\tau^2 + \tau^2\})$, where $\Lambda = \sinh(\tau\sqrt{\ln 4})/(\sigma\tau\sqrt{\ln 4})$, the peak position is m_0 , the width is σ , and τ is the tail parameter.
- [15] E. Bloom and C. Peck, *Annu. Rev. Nucl. Part. Sci.* **33**, 143 (1983).
- [16] *BABAR* Collaboration, B. Aubert *et al.*, *Phys. Rev. D* **69**, 071101 (2004).
- [17] Particle Data Group, K. Hagiwara *et al.*, *Phys. Rev. D* **66**, 010001 (2002).
- [18] *BABAR* Collaboration, B. Aubert *et al.*, *Phys. Rev. Lett.* **92**, 241802 (2004).
- [19] *BABAR* Collaboration, B. Aubert *et al.*, *Phys. Rev. Lett.* **93**, 021804 (2004).